

## Article

# Study on the Preparation of ZnFeO<sub>4</sub> by Roasting Zinc-Containing Gossan Ore

Jinlin Yang<sup>1</sup>, Zongyu Li<sup>1</sup>, Xingnan Huo<sup>1</sup>, Hangyu Li<sup>1</sup>, Shizhen Liao<sup>1</sup>, Shaojian Ma<sup>1</sup> and Hengjun Li<sup>2,\*</sup>

<sup>1</sup> State Key Laboratory of Featured Metal Materials and Life-Cycle Safety for Composite Structures, MOE Key Laboratory of New Processing Technology for Nonferrous Metals, Guangxi Higher School Key Laboratory of Minerals Engineering and Materials, College of Resources, Environment and Materials, Guangxi University, Nanning 530004, China; 2215394008@st.gxu.edu.cn (H.L.)

<sup>2</sup> College of Chemistry and Chemical Engineering, Guangxi University, Nanning 530004, China

\* Correspondence: 1615302001@st.gxu.edu.cn; Tel.: +86-131-5266-0958

**Abstract:** Gossan ore is typically abandoned after mining, which not only increases mining production costs but also wastes mineral resources, and its long-term accumulation can easily lead to environmental pollution hazards. Therefore, this paper takes zinc-containing gossan ore as the research object and, based on the high content of zinc and iron minerals in gossan ore, this study conducts a roasting experiment to prepare ZnFeO<sub>4</sub>. X-ray diffraction is used to characterize and analyze the ZnFeO<sub>4</sub> sample prepared by roasting zinc-containing gossan ore. The experimental results indicate that controlling the particle size of the roasted ore sample to  $-0.074$  mm can effectively remove impurities and facilitate the reaction. The influence of roasting temperature and time on the formation of ZnFeO<sub>4</sub> is remarkable. The conditions for roasting zinc-containing gossan ore to maximize the ZnFeO<sub>4</sub> content are as follows:  $-0.074$  mm particle size ore sample, reaction zinc/iron molar ratio of 1:2, mechanical activation time of 120 min, roasting temperature of 1050 °C, and roasting time of 120 min. These findings provide new ideas for the utilization of gossan ore and lay a theoretical foundation for the efficient development and utilization of difficult-to-select zinc-containing gossan ore.



**Citation:** Yang, J.; Li, Z.; Huo, X.; Li, H.; Liao, S.; Ma, S.; Li, H. Study on the Preparation of ZnFeO<sub>4</sub> by Roasting Zinc-Containing Gossan Ore. *Processes* **2023**, *11*, 1991. <https://doi.org/10.3390/pr11071991>

Academic Editors: Ping Gao, Yidong Cai, Yingfang Zhou and Quan Gan

Received: 15 June 2023

Revised: 26 June 2023

Accepted: 27 June 2023

Published: 1 July 2023



**Copyright:** © 2023 by the authors. Licensee MDPI, Basel, Switzerland. This article is an open access article distributed under the terms and conditions of the Creative Commons Attribution (CC BY) license (<https://creativecommons.org/licenses/by/4.0/>).

**Keywords:** gossan ore; ZnFeO<sub>4</sub>; roasting; preparation

## 1. Introduction

Gossan ore, as a mineral resource, has typically been overlooked by researchers due to its complex composition, low valuable metal content, and high development costs. The mineral and chemical composition of gossan ore is related to the main metal components in the primary sulfide deposit. Various types of primary sulfide deposits form gossans through surface oxidation, and their elemental combinations differ [1]. For example, gossan ore formed from sulfide ore deposits containing gold (silver) contains valuable metals such as gold (silver) and iron. The valuable metals of iron ore in sulfide copper deposits include copper and iron, whereas those in gossan ore of sulfide zinc deposits include zinc and iron. These gossan ores contain many valuable metals and have considerable potential for development and utilization. From the perspective of mineral resource sustainability, with the gradual depletion of high-quality mineral resources, resources such as gossan ore are bound to be effectively utilized in the future to compensate for the shortage of mineral resources. Therefore, gossan ore exhibits immense potential for recycling value. However, although there are several valuable metals in gossan ore, due to its oxidized nature and low metal content, conventional beneficiation and smelting techniques are difficult to effectively recover and utilize resources. For decades, gossan has been limited in its application as a guide for exploring deep sulfide ore bodies, especially those containing Cu, Pb, Zn, Mo, Ni, Au, and Pt [2,3]. As a result, studies on the application of gossan ore remain scarce, with the studies being limited to investigating the use of gossan ore in determining the type and

content of ore deposits [4–6], the heavy metal composition in gossan ore and its impact on the surrounding environment [7–10], and the high value-added precious metal gold (silver) in gossan ore [11–13]. In summary, research on the development and utilization of gossan ore primarily focuses on the recovery of gold, silver, and copper, with limited research efforts being dedicated toward the development and utilization of other valuable elements in gossan ore.

ZnFeO<sub>4</sub> is an excellent material with a stable structure and does not easily decompose at high temperatures. It is nontoxic and harmless to the human body and insoluble in weak acids and alkalis. Utilizing these excellent properties of ZnFeO<sub>4</sub>, high-temperature and corrosion-resistant nontoxic coatings can be prepared. ZnFeO<sub>4</sub> also exhibits excellent photocatalytic performance and can be used for the catalytic adsorption and degradation of water pollutants. Furthermore, ZnFeO<sub>4</sub> is highly sensitive to visible light, does not undergo photocorrosion, and possesses interface electron transfer characteristics, making it an excellent photoelectric conversion material [14–18]. Ebrahimi prepared ZnFeO<sub>4</sub> nanoparticles with a mixed spinel structure using the coprecipitation method at 20–80 °C [19]. Sangita et al. summarized various manufacturing methods of ZnFeO<sub>4</sub> [20]. Sun investigated the preparation of mesoporous ZnFeO<sub>4</sub> flame retardants at different scales and their performance in epoxy resins [21]. Rachna investigated the preparation, characterization, performance, and application of nano ZnFeO<sub>4</sub> [22]. These researchers used high-purity raw materials to prepare ZnFeO<sub>4</sub>, which has high costs and low economic benefits.

Therefore, based on the new concepts of material processing technology for mineral resources, this study innovatively proposes a technical concept of preparing ZnFeO<sub>4</sub> from zinc-containing gossan ore. This concept is based on the high content of zinc and iron minerals in zinc-containing gossan ore. By adjusting the phase of zinc and iron minerals in the ore and applying roasting methods, ZnFeO<sub>4</sub> products are synthesized. This study lays a theoretical groundwork for the development of new processes and technologies for the preparation of ZnFeO<sub>4</sub> with industrial application value, as well as the efficient development and utilization of zinc-containing gossan ore.

## 2. Materials and Methods

### 2.1. Materials

The test sample was a zinc-containing gossan ore extracted from a certain mine, as depicted in Figure 1.



**Figure 1.** Raw gossan ore sample.

As shown in Figure 1, the gossan ore had an irregular block shape and an earthy yellow or brown surface with many corrosion traces. The surface of the ore had irregularly distributed small pores, consistent with the appearance characteristics of classic gossan ore. The zinc-containing gossan ore was dried naturally, crushed, and screened to obtain a –1-mm test sample, following which it was mixed well and bagged for subsequent testing. The crushing equipment was a jaw crusher, model XPC-100 × 150, and the screening equipment was a vibrating screen, model Analysette 3.

The semiquantitative multi-element analysis results of gossan ore are presented in Table 1. The equipment was an X-ray fluorescence element analyzer, model S8 TIGER.

**Table 1.** The multi-element semiquantitative analysis results of gossan ore (source: [23]).

Component	Zn	Fe <sub>2</sub> O <sub>3</sub>	SiO <sub>2</sub>	Al <sub>2</sub> O <sub>3</sub>	MgO	CaO
Content (%)	8.99	68.32	10.32	5.6	1.35	0.56
Component	Na <sub>2</sub> O	K <sub>2</sub> O	SO <sub>3</sub>	TiO <sub>2</sub>	Mn	Pb
Content (%)	0.20	0.12	0.90	0.25	1.46	1.38

Table 1 shows that the chemical element composition of the sample was simple and was mainly composed of zinc, iron, silicon, oxygen, and aluminum. Furthermore, there were trace amounts of metal elements such as manganese, magnesium, calcium, and lead. The main components of the ore were zinc minerals, iron minerals, silica, and alumina, with Zn accounting for 8.99%, Fe<sub>2</sub>O<sub>3</sub> for 68.32%, SiO<sub>2</sub> for 10.32%, and Al<sub>2</sub>O<sub>3</sub> for 5.6% of the ore.

## 2.2. Experimental Principles and Characterization Methods

### 2.2.1. Test Methods and Principles

This study adopted the roasting method to prepare ZnFeO<sub>4</sub>. The effects of factors such as material particle size, mechanical activation time, roasting temperature, and roasting time were studied. The specific test method was as follows.

First, a GD200 × 75 planetary grinding ball mill was used to finely grind the −1 mm-particle size gossan ore sample, and a test sample with a particle size of −0.074 mm was screened out. Second, zinc and iron assays were conducted on samples with a particle size of −0.074 mm to obtain the zinc/iron molar ratio in the gossan ore. Then, based on the zinc/iron molar ratio in the gossan ore and the zinc/iron molar ratio required by the ZnFeO<sub>4</sub> reaction theory, zinc or iron oxide was added to regulate the appropriate zinc/iron molar ratio. Then, the test sample with an adjusted zinc/iron molar ratio was placed into the GD200 × 75 planetary grinding ball mill for mechanical activation treatment. Finally, the mechanically activated test samples were taken and roasted in a GXL-15 high-temperature box furnace to obtain the roasted ZnFeO<sub>4</sub> product.

The main chemical reactions that may occur during the roasting process for preparing ZnFeO<sub>4</sub> are as follows:



### 2.2.2. Characterization Methods

X-ray diffraction (XRD) analysis was the main method used in the experiment for characterization and analysis, and the analysis principle is as follows.

In XRD analysis, the intensity of the diffraction rays of different substances in a mixture increases with the relative content of the substance in the sample. As a result, the diffraction peak intensity of ZnFeO<sub>4</sub> in XRD analysis can be used to calculate the relative content of ZnFeO<sub>4</sub> in the sample.

## 3. Results and Discussion

### 3.1. Effect of Ore Particle Size

Here, the research on the effect of ore particle size is primarily based on two considerations. First, one of the main impurity minerals of gossan ore is quartz, with a Mohs hardness of 7.0, whereas the Mohs hardness of smithsonite in the main zinc and iron ores is 4–4.5, that of hemimorphite is 4–4.5, and that of limonite is 1–4. The hardness of impurity mineral quartz is higher than that of zinc and iron minerals; thus, fine grinding and screening may be performed to remove some difficult-to-grind quartz. Second, the specific surface area of materials with different particle sizes differs, affecting the reaction rate. Therefore, the effect of ore particle size on the preparation of ZnFeO<sub>4</sub> by roasting

was investigated. After grinding the  $-1$  mm gossan ore sample for 1 h, the samples were sieved using 150-, 180-, 200-, and 250-mesh sieves. The corresponding particle sizes of the products under the sieves were  $-0.1$ ,  $-0.088$ ,  $-0.074$ , and  $-0.065$  mm, respectively. The other experimental conditions are as follows: zinc/iron molar ratio of 1:2, mechanical activation time of 120 min, roasting temperature of  $1050$  °C, and roasting time of 120 min. The content of  $\text{ZnFeO}_4$  in products roasted with different particle sizes is shown in Table 2.

**Table 2.** Content of  $\text{ZnFeO}_4$  in roasted products of different particle sizes.

Particle Size (mm)	$-1$	$-0.1$	$-0.088$	$-0.074$	$-0.065$
Content of $\text{ZnFeO}_4$ (%)	75.3	80.1	85.3	88.6	88.4

Table 2 shows that as the particle size of zinc-containing gossan ore decreased, the amount of  $\text{ZnFeO}_4$  generated continuously increased; however, there was negligible change after the  $-0.074$  mm particle size. Among them, the  $\text{ZnFeO}_4$  content in the roasted product of  $-1$  mm particle size was 75.3%, whereas the  $\text{ZnFeO}_4$  content in the roasted product of  $-0.074$  mm particle size was 88.6%, and the  $\text{ZnFeO}_4$  content was increased by 13.3%.

The multi-element semiquantitative analysis results of the  $-0.074$  mm particle size sample are shown in Table 3.

**Table 3.** The multi-element semiquantitative analysis results of the  $-0.074$  mm particle size sample.

Component	Zn	$\text{Fe}_2\text{O}_3$	$\text{SiO}_2$	$\text{Al}_2\text{O}_3$	MgO	CaO
Content (%)	12.32	73.56	5.81	2.6	0.78	0.68
Component	$\text{Na}_2\text{O}$	$\text{K}_2\text{O}$	$\text{SO}_3$	$\text{TiO}_2$	Mn	Pb
Content (%)	0.15	0.10	0.86	0.35	0.96	1.45

Tables 1 and 3 illustrate that after fine grinding and screening with a 200-mesh sieve, the silicon dioxide content in the  $-0.074$  mm particle size ore sample considerably decreased by approximately 43.7%. Therefore, the relative content of zinc and iron minerals as reactants also increased to a certain extent, which was conducive to the formation of  $\text{ZnFeO}_4$  and increased the  $\text{ZnFeO}_4$  content in the roasted product.

XRD analysis was performed on the products after roasting the samples with particle sizes of  $-1$ ,  $-0.1$ ,  $-0.088$ ,  $-0.074$ , and  $-0.065$  mm. The XRD diffraction patterns are displayed in Figure 2.

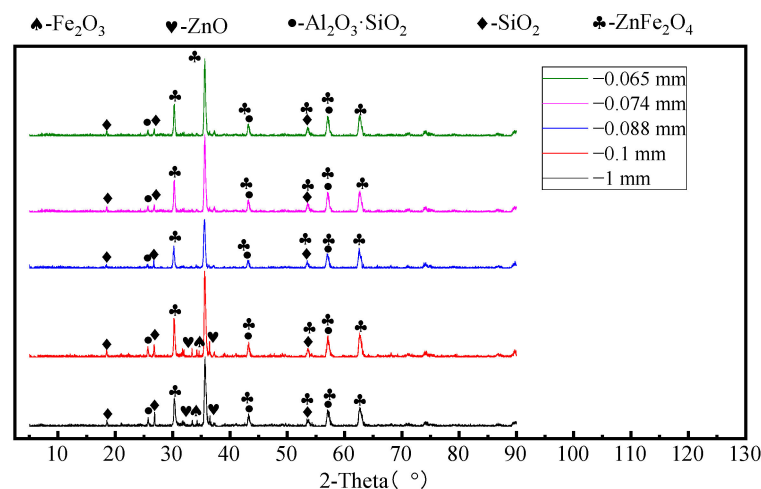


**Figure 2.** XRD patterns of the roasted products at different particle sizes.

Figure 2 shows that among the five roasted ore products, the diffraction peaks of silicon and aluminum compounds in the roasted products with  $-1$  and  $-0.1$  mm particle sizes exhibited almost no change in intensity, indicating that the use of a 150-mesh sieve did not substantially remove silicon and aluminum minerals. After sieving with a 180-mesh or finer sieve, silicon and aluminum minerals can be effectively removed. A comparison of the roasted products with particle sizes of  $-0.074$  and  $-0.065$  mm revealed that the diffraction peaks of silicon and aluminum compounds were the smallest. However, the difference between the two was insignificant. Therefore, the subsequent experimental ore samples were selected as follows: the original  $-0.1$  mm particle size gossan ore was finely ground for 1 h and screened with a 200-mesh sieve, and the  $-0.074$  mm particle size ore sample was used as the material to prepare  $\text{ZnFe}_2\text{O}_4$ .

### 3.2. Effect of Roasting Temperature

The roasting temperature test conditions were  $-0.074$  mm particle size ore sample; zinc/iron molar ratio of 1:2; mechanical activation time of 120 min; roasting time of 120 min; and roasting temperatures of  $700$  °C,  $800$  °C,  $900$  °C,  $1050$  °C, and  $1200$  °C, respectively. The XRD patterns of the roasted products at different roasting temperatures are depicted in Figure 3.

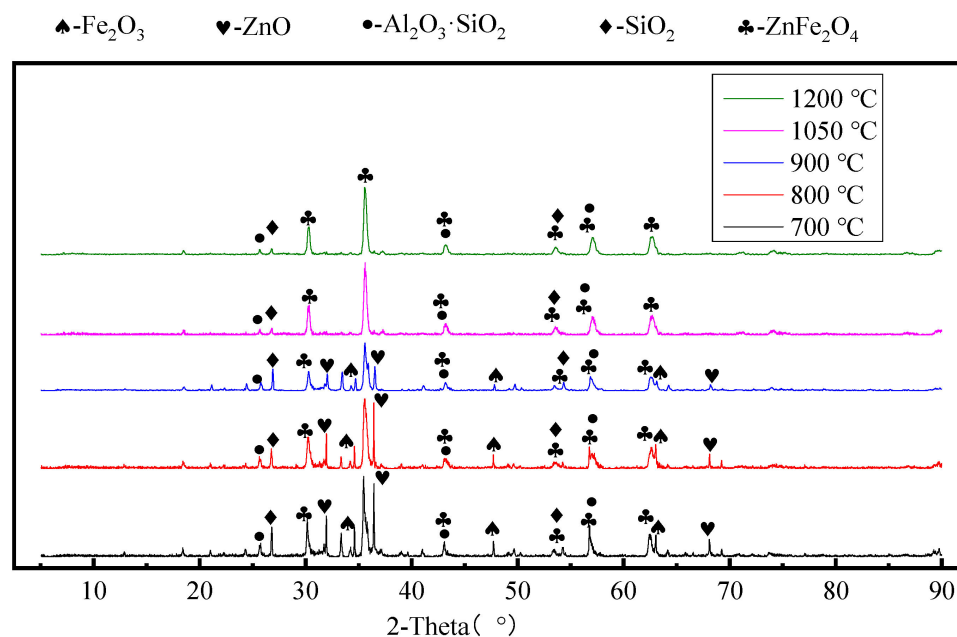
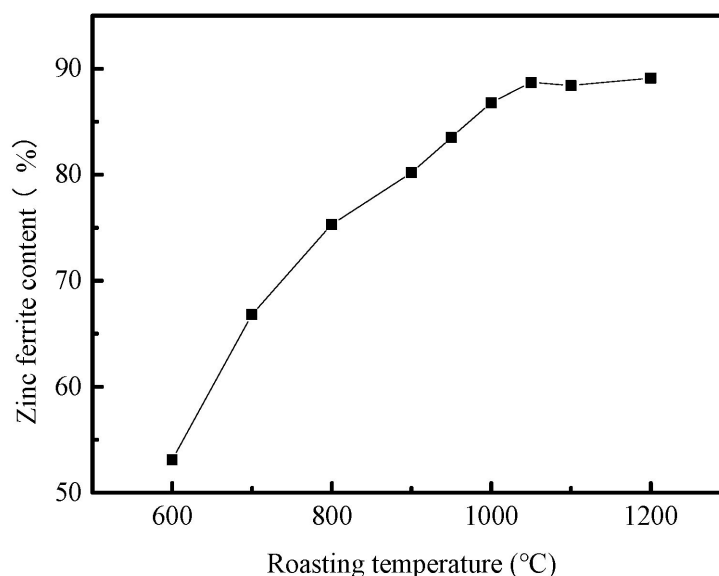


Figure 3. XRD patterns of the roasted products at different roasting temperatures.

Figure 3 shows that at roasting temperatures of  $700$  °C and  $800$  °C, the diffraction peaks of zinc and iron oxide minerals strengthened, indicating that several reactants had yet to undergo the reaction. When the roasting temperature reached  $900$  °C, the diffraction peaks of zinc and iron oxide minerals weakened, indicating that at this roasting temperature, the reactant content in the sample decreased and the reaction proceeded more fully. When the roasting temperature increased from  $700$  °C to  $900$  °C, the diffraction peak intensity represented by zinc oxide minerals in the XRD pattern exhibited the largest decrease, and the diffraction peak of iron oxide minerals also weakened to a certain extent. This indicates that a considerable amount of zinc and iron oxide minerals, such as smithsonite and limonite, participated in the reaction when the roasting temperature increased from  $700$  °C to  $900$  °C. When the roasting temperature was  $1050$  °C, the diffraction peak of  $\text{ZnFe}_2\text{O}_4$  in the roasted product was evident, whereas those of zinc and iron oxide minerals disappeared, indicating that the reaction was complete at this time. When the roasting temperature was above  $1050$  °C, the diffraction curve of the sample remained almost unchanged, and the

diffraction peaks of  $\text{ZnFeO}_4$  were also visible, whereas the diffraction peaks of the zinc and iron oxide minerals disappeared. According to XRD quantitative analysis, the  $\text{ZnFeO}_4$  content in the roasted product reached 75.3% at a roasting temperature of 800 °C. At a roasting temperature of 1050 °C, the  $\text{ZnFeO}_4$  content in the roasted product was 88.6%.

To investigate the changes in  $\text{ZnFeO}_4$  content in roasted products at different roasting temperatures, the following experiments were conducted. The experimental conditions were as follows:  $-0.074$  mm particle size ore sample; zinc/iron molar ratio of 1:2; mechanical activation time of 120 min; roasting time of 120 min; and roasting temperatures of 600 °C, 700 °C, 800 °C, 900 °C, 950 °C, 1000 °C, 1050 °C, 1100 °C, and 1200 °C. The variation in  $\text{ZnFeO}_4$  content among the roasted products with roasting temperature is depicted in Figure 4.



**Figure 4.**  $\text{ZnFeO}_4$  content of the roasted products at different temperatures.

Figure 4 reveals that prior to 1050 °C, the increase in roasting temperature had a remarkable impact on the formation of  $\text{ZnFeO}_4$ , resulting in a rapid increase in  $\text{ZnFeO}_4$  content. After 1050 °C, there was little change in the  $\text{ZnFeO}_4$  content. Therefore, a roasting temperature of approximately 1050 °C is the optimal temperature in terms of maximizing  $\text{ZnFeO}_4$  content. However, a high temperature of 1050 °C consumes a substantial amount of energy, and the higher the temperature, the more time and energy required to raise the temperature. Therefore, from the perspective of saving energy consumption and based on the XRD spectrum analysis in Figure 3, the diffraction peaks of zinc and iron oxide minerals weaken when the roasting temperature reaches 800 °C. At this roasting temperature, the content of reactants in the sample considerably decreases and the reaction proceeds more fully. Therefore, the roasting temperature is a crucial factor affecting the formation of  $\text{ZnFeO}_4$ .

### 3.3. Effect of Mechanical Activation Time

The mechanical activation time test conditions were  $-0.074$  mm particle size ore sample; zinc/iron molar ratio of 1:2; roasting temperatures of 800 °C, 900 °C, 950 °C, 1000 °C, and 1050 °C; roasting time of 120 min; and mechanical activation times of 0, 60, 120, and 200 min. The XRD patterns of the roasted products at different roasting temperatures and mechanical activation times are depicted in Figure 5.

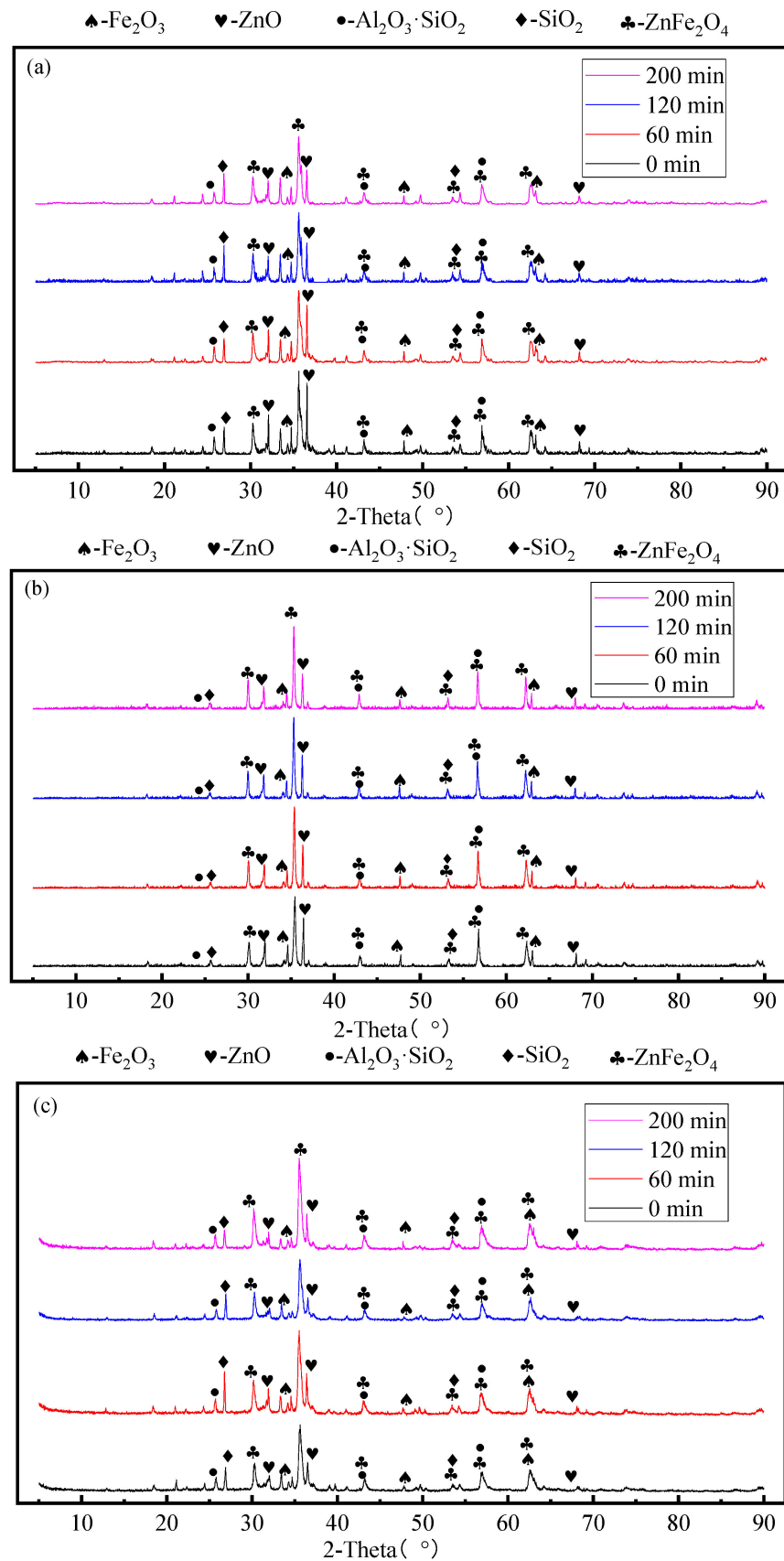
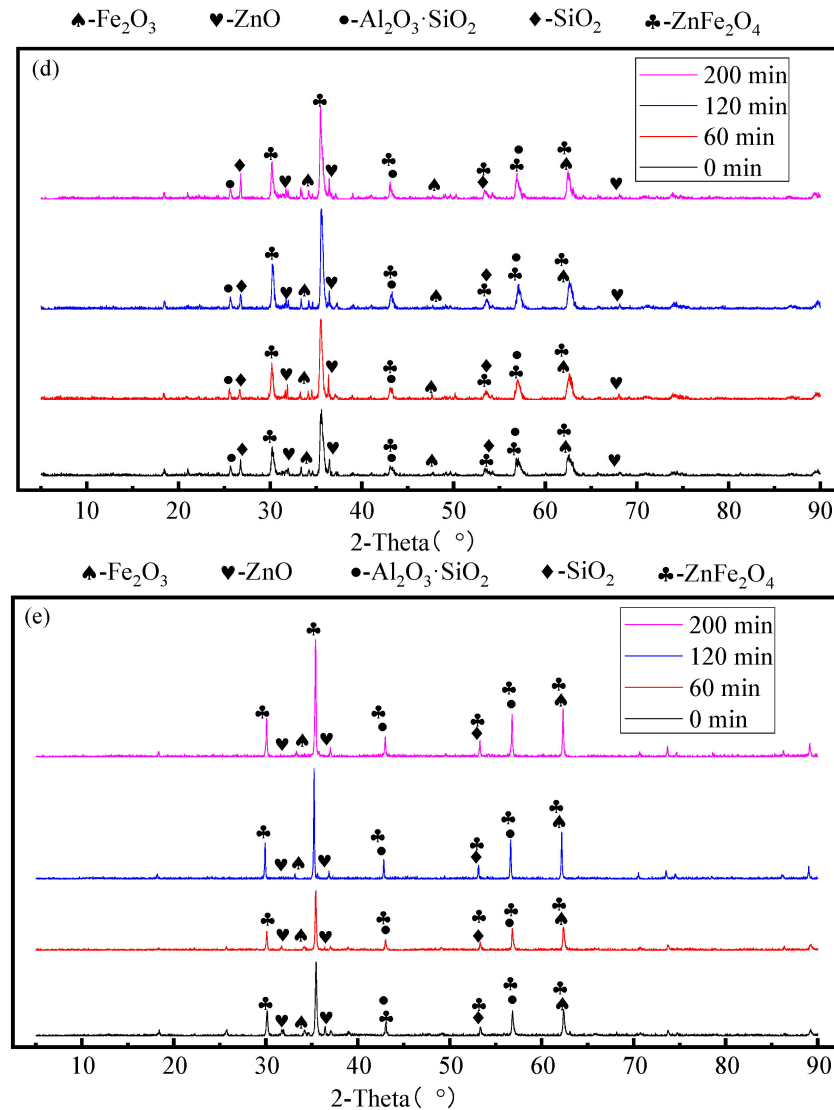


Figure 5. Cont.



**Figure 5.** XRD patterns of the roasted products at different roasting temperatures and mechanical activation times: (a): 800 °C; (b): 900 °C; (c): 950 °C; (d): 1000 °C; (e): 1050 °C.

Figure 5a illustrates that at a roasting temperature of 800 °C, with prolonging mechanical activation time, the diffraction peak of ZnFeO<sub>4</sub> in the roasted product strengthened, indicating an increase in the ZnFeO<sub>4</sub> content. XRD quantitative analysis revealed that the content of ZnFeO<sub>4</sub> in the roasted product increased from 68.4% under 0 min mechanical activation to 75.3% under 120 min mechanical activation. This may be attributed to the fact that during mechanical activation, the ore produces several lattice dislocations at a microscopic level. The aggregation of many lattice dislocations can generate microcracks. The rapid propagation of these microcracks results in a temperature exceeding 1300 K at the top of the crack. On a microscopic scale, the high-temperature and high-pressure state at the top of the crack corresponds to the high-speed movement of atoms, promoting the migration and diffusion between atoms, which is conducive to the progress of the reaction. Furthermore, some atoms are excited, and electrons are excited in extremely small regions to form a plasma region, further accelerating the reaction. In addition, mechanical activation plays a role in the ability to completely crush and grind the material, increasing the specific surface area of the sample and the possibility of direct contact between the reaction materials, thereby effectively improving the reaction rate. A comparison of Figure 5a–e reveals that the increase in roasting temperature led to a considerable enhancement in the diffraction peak of ZnFeO<sub>4</sub> in the XRD spectrum of the sample. However, when the

roasting temperature exceeded 1000 °C, the XRD spectrum of the roasted sample exhibited little change under different mechanical activation times, indicating that the promotion effect of mechanical activation on the preparation of ZnFeO<sub>4</sub> by roasting was insignificant at this temperature.

To investigate the effect of mechanical activation time on the preparation of ZnFeO<sub>4</sub> at different roasting temperatures, the following experiments were conducted. The experimental conditions were −0.074 mm particle size ore sample; zinc/iron molar ratio of 1:2; roasting temperatures of 800 °C, 900 °C, 950 °C, 1000 °C, and 1050 °C; roasting time of 120 min; and mechanical activation times of 0, 30, 60, 90, 120, 150, and 200 min. The effect of mechanical activation time on the content of ZnFeO<sub>4</sub> in the roasted products at different roasting temperatures is depicted in Figure 6.

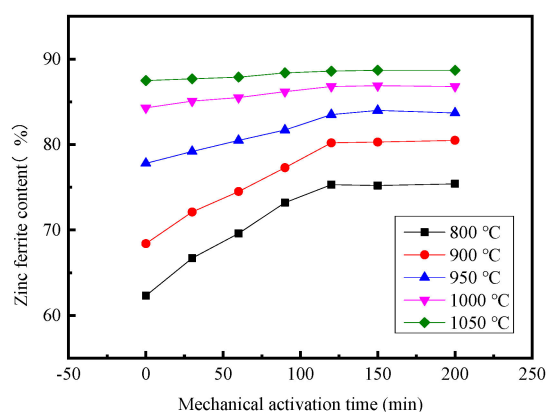


**Figure 6.** Effect of mechanical activation time on ZnFeO<sub>4</sub> content of the roasted products at different roasting temperatures.

Figure 6 shows that at a roasting temperature of 800 °C, the mechanical activation time had a remarkable impact on the ZnFeO<sub>4</sub> content in the roasted product. According to the analysis results, the ZnFeO<sub>4</sub> content was 62.3% in the absence of mechanical activation. After 120 min of mechanical activation, the ZnFeO<sub>4</sub> content in the roasted product reached 75.3%, demonstrating an increase of 13% compared with the case of ZnFeO<sub>4</sub> content without mechanical activation. At a roasting temperature of 900 °C, the content of ZnFeO<sub>4</sub> is 68.4% without mechanical activation. After 120 min of mechanical activation, the content of ZnFeO<sub>4</sub> in the roasted product reached 80.2%. Consequently, the content of ZnFeO<sub>4</sub> increased by 11.8%, which was lower than the increase in ZnFeO<sub>4</sub> content at 800 °C. At higher roasting temperatures of 1000 °C and 1050 °C, the effect of mechanical activation time on the preparation of ZnFeO<sub>4</sub> by roasting was insignificant. According to the analysis results, within the range of the above mechanical activation times, the highest ZnFeO<sub>4</sub> content in the sample was approximately 86.8% at a roasting temperature of 1000 °C, whereas the highest ZnFeO<sub>4</sub> content in the sample was approximately 88.6% at a roasting temperature of 1050 °C. This could be attributed to the roasting temperature being sufficiently high for the −0.074 mm particle size sample and the particles being capable of completely diffusing. At this time, mechanical activation has marginal utility. Because the reactants could fully react under a short mechanical activation time, extending the mechanical activation time has no considerable impact on the formation of ZnFeO<sub>4</sub>. This further elucidates the point that roasting temperature is a crucial factor affecting the formation of ZnFeO<sub>4</sub>.

### 3.4. Effect of Roasting Time

The roasting time test conditions were −0.074 mm particle size ore sample; zinc/iron molar ratio of 1:2; mechanical activation time of 120 min; roasting temperatures of 800 °C, 900 °C, 950 °C, 1000 °C, and 1050 °C; and roasting times of 30, 60, 90, 120, and 150 min. The XRD patterns of the roasted products at different roasting temperatures and times are depicted in Figure 7.

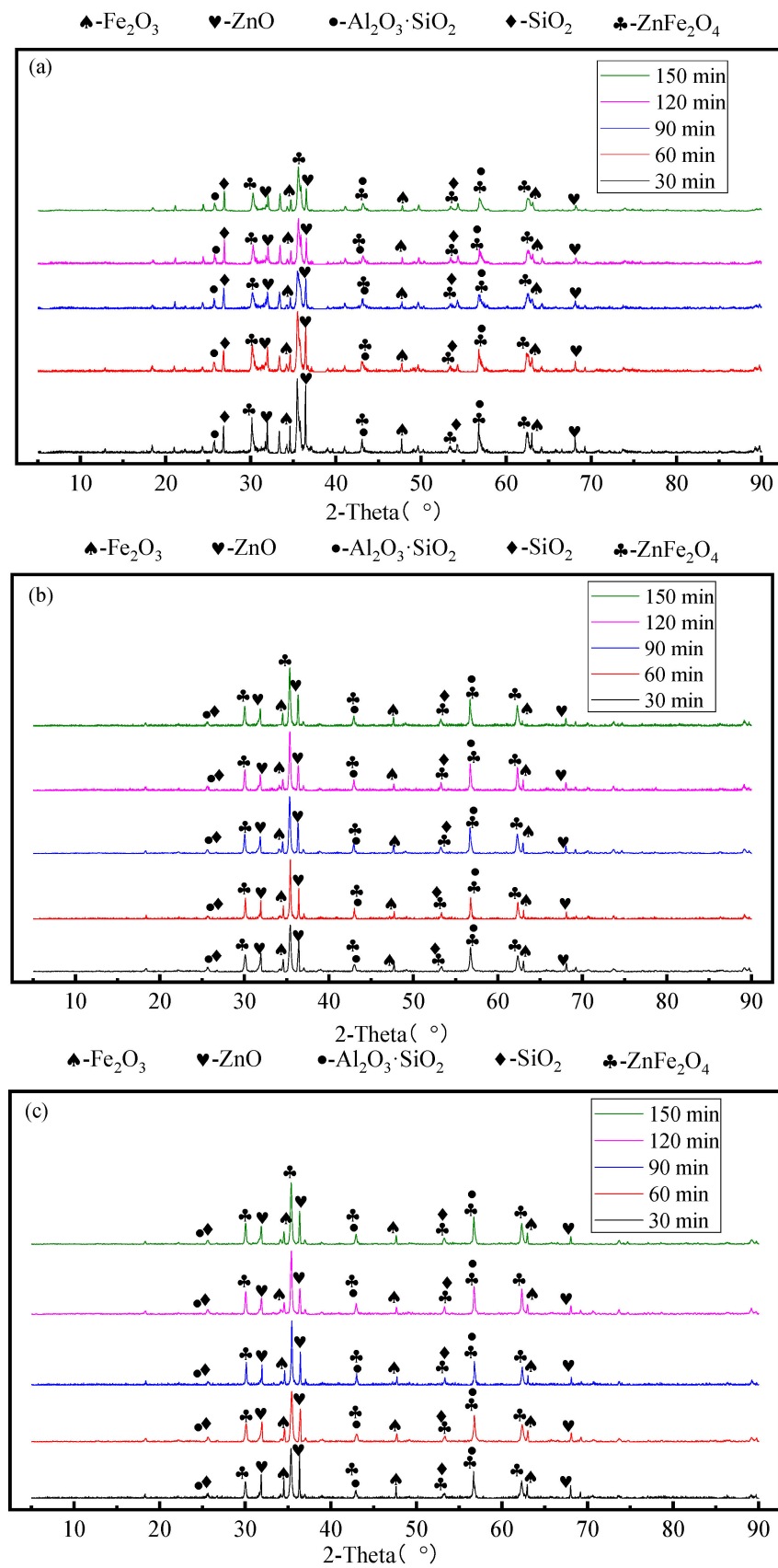
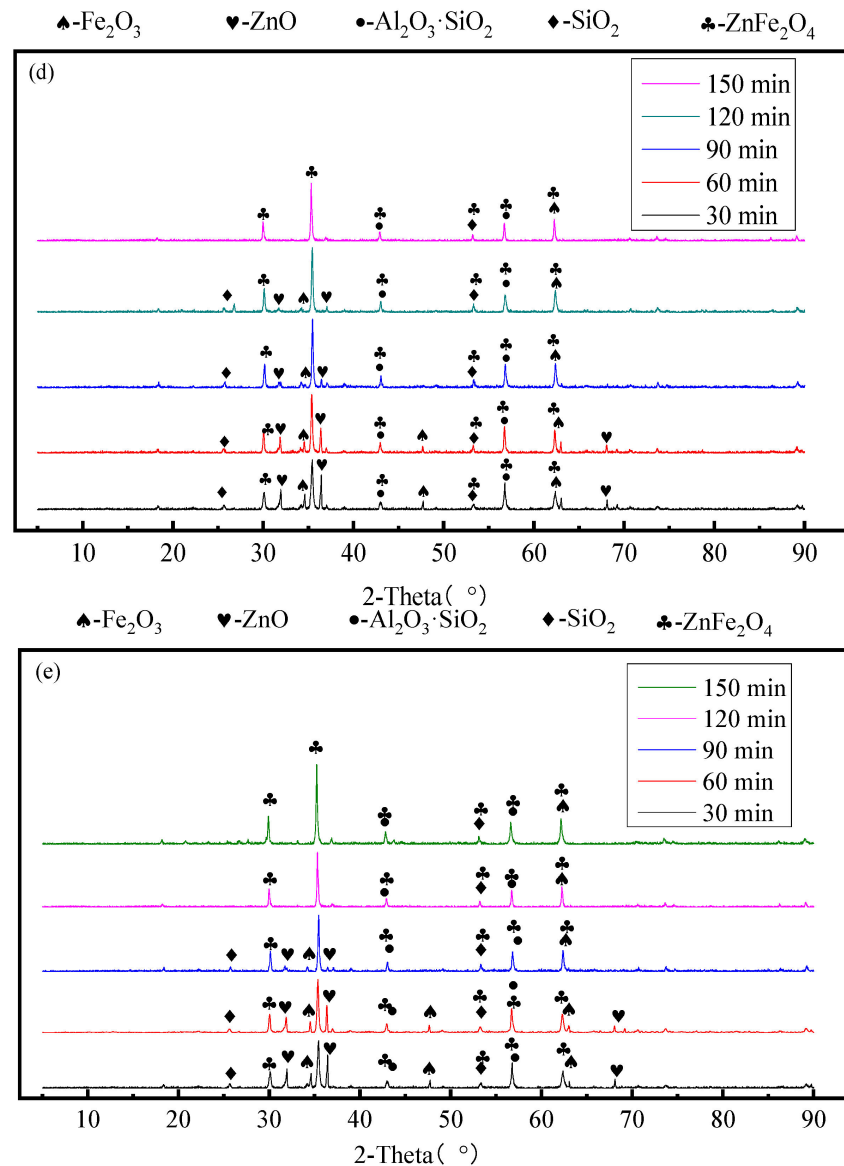


Figure 7. Cont.



**Figure 7.** XRD patterns of the roasted products at different roasting times and temperatures: (a): 800 °C; (b): 900 °C; (c): 950 °C; (d): 1000 °C; (e): 1050 °C.

Figure 7 shows that for roasting times of 30 and 60 min, within the experimental roasting temperature range, the diffraction peaks of iron and zinc oxides in all roasted products were evident to a larger degree, indicating a considerable amount of unreacted reactants in the sample. After the roasting time reached 90 min, the diffraction peaks of zinc and iron oxides in the roasted products at 1000 °C and 1050 °C considerably weakened, indicating a complete reaction. At roasting temperatures above 1000 °C, the roasting time was extended, and the ZnFeO<sub>4</sub> content was substantially increased within the 30–90 min roasting time range. When the roasting time was 120 min, the diffraction peaks of iron and zinc oxides were weak, whereas those of ZnFeO<sub>4</sub> were strong. When the roasting time reached 120 min, the reaction was complete. When the roasting time was 150 min, in a manner similar to that when the roasting time was 120 min, there were almost no diffraction peaks of zinc and iron oxides, but the diffraction peaks of ZnFeO<sub>4</sub> were very strong, indicating that the reaction was sufficient at this time. Note that the XRD-pattern waveforms of the samples for roasting times of 120 and 150 min are very similar. Because the diffraction peak intensity of a substance represents the relative content of the substance, the peaks of the spectra of the samples are similar, indicating that the reaction was complete.

at this time. Moreover, the peak diffraction intensity of  $\text{ZnFeO}_4$  was high, and the difference was insignificant, indicating that the  $\text{ZnFeO}_4$  content in the samples was high. At roasting temperatures of 800 °C and 900 °C and roasting time of 90 min or more, the diffraction peak of zinc/iron impurities in the sample was evident. This indicates that the reaction of zinc-containing gossan ore was not fully complete at this temperature and the roasted product contained many impurities.

To investigate the effect of roasting time at different roasting temperatures on the formation of  $\text{ZnFeO}_4$ , the following experiments were conducted. The experimental conditions were as follows:  $-0.074$  mm particle size ore sample; zinc/iron molar ratio of 1:2; mechanical activation time of 120 min; roasting temperatures of 800 °C, 900 °C, 950 °C, 1000 °C, and 1050 °C; and roasting times of 30, 45, 60, 75, 90, 105, 120, 135, 150, 165, and 180 min. The effect of roasting time at different roasting temperatures on the preparation of  $\text{ZnFeO}_4$  is depicted in Figure 8.

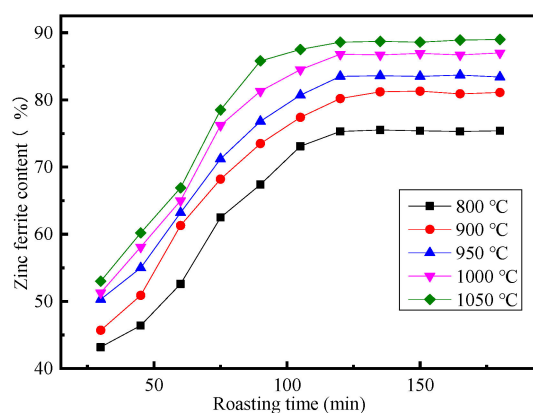


**Figure 8.** Effect of roasting time on  $\text{ZnFeO}_4$  content of the roasted products at different roasting temperatures.

Figure 8 shows that at low roasting temperatures (800 °C and 900 °C) and a roasting time of less than 75 min, the  $\text{ZnFeO}_4$  content in the roasted product increased rapidly, exhibiting a near-linear trend. When the roasting time was 75–105 min, the growth rate of the zinc ferrite content slowed. When the roasting time was above 120 min, the  $\text{ZnFeO}_4$  content in the roasted product remained almost unchanged. At high roasting temperatures (1000 °C and 1050 °C), the pattern exhibited was similar to that at lower roasting temperatures, except for the faster growth rate of  $\text{ZnFeO}_4$  in the early stage. When the roasting time reached 120 min, the  $\text{ZnFeO}_4$  content was almost maximum. If the roasting time was extended further, the  $\text{ZnFeO}_4$  content in the product would not change considerably, indicating that the sample had fully reacted at this time. Figure 8 also shows that at a roasting time above 120 min, the  $\text{ZnFeO}_4$  content in the roasted products at different roasting temperatures reached equilibrium. Moreover, as the roasting temperature increased, the slope of the curve also slightly increased, indicating that higher roasting temperatures lead to a faster increase in  $\text{ZnFeO}_4$  content.

#### 4. Conclusions

(1) Before roasting, fine grinding and screening of the  $-1$  mm gossan ore sample can effectively remove impurities and facilitate the reaction by controlling the particle size of the ore to  $-0.074$  mm. Compared with nonscreening after fine grinding of the ore, the  $\text{ZnFeO}_4$  content in the roasted product increased by 13.3% after roasting for a particle size of  $-0.074$  mm.

(2) When the roasting temperature was low (800 °C), the mechanical activation time had a remarkable impact on the preparation of  $\text{ZnFeO}_4$  by roasting. Following 120 min mechanical activation, the  $\text{ZnFeO}_4$  content in the roasted product reached 75.3%, which was 13% higher than that without mechanical activation. When the roasting temperature

was high (1050 °C or above), the effect of mechanical activation time on the formation of ZnFeO<sub>4</sub> during roasting was insignificant.

(3) Roasting temperature and roasting time considerably influenced the formation of ZnFeO<sub>4</sub>. As the roasting temperature and roasting time increased, the ZnFeO<sub>4</sub> content in the roasted products gradually increased. When the roasting temperature reached 1050 °C or above and the roasting time reached 120 min, the reaction was complete.

(4) Considering the maximization of ZnFeO<sub>4</sub> content, the suitable conditions for preparing ZnFeO<sub>4</sub> from zinc-containing gossan ore by roasting are as follows: −0.074 mm-particle size ore sample, reaction zinc/iron molar ratio of 1:2, mechanical activation time of 120 min, roasting temperature of 1050 °C, and roasting time of 120 min. Under these conditions, the ZnFeO<sub>4</sub> content in the roasted product reached 88.6%.

(5) From the perspective of saving energy consumption and simplifying the phase composition of reaction products, the suitable conditions for preparing ZnFeO<sub>4</sub> from zinc-containing gossan ore by roasting are as follows: −0.074 mm particle size ore sample, reaction zinc/iron molar ratio of 1:2, mechanical activation time of 120 min, roasting temperature of 800 °C, and roasting time of 120 min. Under these conditions, the ZnFeO<sub>4</sub> content in the roasted product reached 75.3%.

**Author Contributions:** Conceptualization, J.Y. and Z.L.; data curation, Z.L. and H.L. (Hengjun Li); formal analysis, X.H. and S.L.; funding acquisition, J.Y.; investigation, S.L. and H.L. (Hangyu Li); methodology, J.Y. and S.M.; project administration, J.Y. and H.L. (Hengjun Li); validation, H.L. (Hengjun Li) and Z.L.; writing—original draft, H.L. (Hengjun Li) and Z.L.; writing—review and editing, J.Y. and S.M. All authors have read and agreed to the published version of the manuscript.

**Funding:** This research was funded by the National Natural Science Foundation of China (No. 52264020, No. 51774099).

**Data Availability Statement:** Not applicable.

**Conflicts of Interest:** The authors declare no conflict of interest.

## References

- Pablllo, H.C.S.; Marcondes, L.C. Mineralogical and textural evolution of the Alvo 118 copper-bearing gossan: Implications for supergene metallogenesis in Carajás Mineral Province. *Brazil. J. S. Am. Earth Sci.* **2023**, *121*, 104108.
- Andreu, E.; Torró, L.; Proenza, J.A.; Domenech, C.; García-Casco, A.; Villanova de Benavent, C.; Chavez, C.; Espaillet, J.; Lewis, J.F. Weathering profile of the Cerro de Maimón VMS deposit (Dominican Republic): Textures, mineralogy, gossan evolution and mobility of gold and silver. *Ore Geol. Rev.* **2015**, *65*, 165–179. [[CrossRef](#)]
- Pires, G.L.C.; Renac, C.; Bongioiolo, E.M.; Neumann, R. Gossan mineralogy, textures, and gold enrichment over the Au (As, Bi, Ag) deposit in the Buracão Area (Brasília Fold Belt, Brazil): Implications for gold prospecting in weathering profiles. *J. Geochem. Explor.* **2020**, *218*, 106615. [[CrossRef](#)]
- Kříbek, B.; Zachariáš, J.; Knésl, I.; Míková, J.; Mihaljevič, M.; Veselovský, F.; Bamba, O. Geochemistry, mineralogy, and isotope composition of Pb, Zn, and Cu in primary ores, gossan and barren ferruginous crust from the Perkoa base metal deposit, Burkina Faso. *J. Geochem. Explor.* **2016**, *168*, 49–64. [[CrossRef](#)]
- Baggio, S.B.; Hartmann, L.A.; Massonne, H.J.; Theye, T.; Antunes, L.M. Silica gossan as a prospective guide for amethyst geode deposits in the Ametista do Sul mining district, Paraná volcanic province, southern Brazil. *J. Geochem. Explor.* **2015**, *159*, 213–226. [[CrossRef](#)]
- Yesares, L.; Sáez, R.; Ruiz De Almodóvar, G.R.; Nieto, J.M.; Gómez, C.; Ovejero, G. Mineralogical evolution of the Las Cruces gossan cap (Iberian Pyrite Belt): From subaerial to underground conditions. *Ore Geol. Rev.* **2017**, *80*, 377–405. [[CrossRef](#)]
- Laakso, K.; Rivard, B.; Rogge, D. Enhanced detection of gossans using hyperspectral data: Example from the Cape Smith Belt of northern Quebec, Canada. *ISPRS J. Photogramm.* **2016**, *114*, 137–150. [[CrossRef](#)]
- Velasco, F.; Herrero, J.M.; Suárez, S.; Yusta, I.; Alvaro, A.; Tornos, F. Supergene features and evolution of gossans capping massive sulphide deposits in the Iberian pyrite Belt. *Ore Geol. Rev.* **2013**, *53*, 181–203. [[CrossRef](#)]
- Costa, M.L.; Angélica, R.S.; Costa, N.C. The geochemical association Au–As–B–(Cu)–Sn–W in latosol, colluvium, lateritic iron crust, and gossan in Carajás, Brazil: Importance for primary ore identification. *J. Geochem. Explor.* **1999**, *67*, 33–49. [[CrossRef](#)]
- Assawincharoenkij, T.; Hauenberger, C.; Ettinger, K.; Sutthirath, C. Mineralogical and geochemical characterization of waste rocks from a gold mine in northeastern Thailand: Application for environmental impact protection. *Environ. Sci. Pollut. Res. Int.* **2018**, *25*, 3488–3500. [[CrossRef](#)]
- Li, J.M. Experimental study on cyanide leaching of a gossan type gold and silver ore in Qinghai. *Gold Sci. Technol.* **2015**, *23*, 88–93. (In Chinese)

12. Celep, O.; Serbest, V. Characterization of an iron oxy/hydroxide (gossan type) bearing refractory gold and silver ore by diagnostic leaching. *Trans. Nonferrous Met. Soc. China* **2015**, *25*, 1286–1297. [[CrossRef](#)]
13. Zhang, R.; Lu, X.C.; Liu, H. Mineral phase transition and heavy metal release during the reduction of iron caps by *Shewanella oneidensis* MR-1. *Bull. Mineral. Rock Geochem.* **2015**, *34*, 316–322. (In Chinese)
14. Hankare, P.P.; Patil, R.P.; Jadhav, A.V.; Garadkar, K.M.; Sasikala, R. Enhanced photocatalytic degradation of methyl red and thymol blue using titania-alumina-zinc ferrite nanocomposite. *Appl. Catal. B* **2011**, *107*, 333–339. [[CrossRef](#)]
15. Jadhav, S.V.; Jinka, K.M.; Bajaj, H.C. Nanosized sulfated zinc ferrite as catalyst for the synthesis of nopol and other fine chemicals. *Catal. Today* **2012**, *198*, 98–105. [[CrossRef](#)]
16. Matinise, N.; Kaviyarasu, K.; Mongwaketsi, N.; Khamlich, S.; Kotsedi, L.; Mayedwa, N.; Maaza, M. Green synthesis of novel zinc iron oxide( $ZnFe_2O_4$ ) nanocomposite via *Moringa oleifera* natural extract for electrochemical applications. *Appl. Surf. Sci.* **2018**, *446*, 66–73. [[CrossRef](#)]
17. Raut, S.D.; Awasarmol, V.V.; Ghule, B.G.; Shaikh, S.F.; Gore, S.K.; Sharma, R.P.; Pawar, P.P.; Mane, R.S.  $\gamma$ -irradiation induced zinc ferrites and their enhanced room-temperature ammonia gas sensing properties. *Mater. Res. Express* **2018**, *5*, 035702. [[CrossRef](#)]
18. Sai, R.; Kulkarni, S.D.; Yamaguchi, M.; Bhat, N.; Shivashankar, S.A. Integrated X-band inductor with a nanoferrite film core. *IEEE Magn. Lett.* **2017**, *8*, 3703904. [[CrossRef](#)]
19. Ebrahimi, M.; Raeisi Shahraki, R.; Seyyed Ebrahimi, S.A.; Masoudpanah, S.M. Magnetic properties of zinc ferrite nanoparticles synthesized by coprecipitation method. *J. Supercond. Nov. Magn.* **2014**, *27*, 1587–1592. [[CrossRef](#)]
20. Sangita, N.P.; Pratik, A.N.; Arvind, V.N.; Shankar, R.T.; Arun, V.B. Preparation techniques for zinc ferrites and their applications: A review. *Mater. Today Proc.* **2022**, *60*, 2194–2208.
21. Sun, X.M.; Li, Z.W.; Li, X.H.; Zhang, Z.J. Preparation of mesoporous zinc ferrite flame retardant with different scales and its performance in epoxy resin. *Polym. Test.* **2022**, *110*, 107549. [[CrossRef](#)]
22. Rachna, S.; Singh, N.B.; Agarwal, A. Preparation, characterization, properties, and applications of nano zinc ferrite. *Mater. Today Proc.* **2018**, *5*, 9148–9155. [[CrossRef](#)]
23. Yang, J.; Zhu, P.; Ma, S. Study on properties of gossan ore from zinc sulfide deposit. *J. Phys. Conf. Ser.* **2021**, *2044*, 012081. [[CrossRef](#)]

**Disclaimer/Publisher's Note:** The statements, opinions and data contained in all publications are solely those of the individual author(s) and contributor(s) and not of MDPI and/or the editor(s). MDPI and/or the editor(s) disclaim responsibility for any injury to people or property resulting from any ideas, methods, instructions or products referred to in the content.